Available online at www.sciencedirect.com
SCIENCE DIRECT
Polymer 47 (2006) 591–601
polymer
www.elsevier.com/locate/polymer

Preparation of planar and oblate particles from emulsion polymerization using polymerizable comb-like branched emulsifiers

Chi-Jung Chang *, Pei-Chun Kao

Department of Chemical Engineering, Feng Chia University, 100, Wenhwa Road, Seatwen, Taichung 40724, Taiwan, ROC

Received 18 August 2005; received in revised form 24 November 2005; accepted 28 November 2005
Available online 20 December 2005

Abstract

This paper presents a method for preparation of planar polymeric microstructures by emulsion polymerization using polymerizable branched emulsifier. Planar, oblate and spherical particles can be prepared by changing the volume and functionality of the hydrophobic tail of the comb-like polymerizable emulsifier, together with altering the monomers. Emulsifiers with bulky tails favored the formation of planar microstructure. The polymerizable emulsifiers were immobilized on the latex particles. Hindered desorption of the emulsifier from the latex improved the latexes' stability and facilitate the formation of planar and oblate particles. The polymerization conversion also depends on the molecular characteristics of the emulsifiers and monomers.

Keywords: Planar particles; Polymerizable emulsifier; Emulsion polymerization

1. Introduction

The emulsifiers are surfactants which play the crucial and versatile role in emulsion polymerization, including the stabilization of the starting emulsion, the particle nucleation and growth, and the stabilization of the final latex [1]. Surfactant micelles and bilayers are the building blocks of most self-assembly structures. The phase structures can be characterized as spherical, prolate, oblate or cylindrical, or infinite self-assemblies. In the latter case, the surfactant aggregate is connected over macroscopic distance in one-, two- or three-dimensions. The hexagonal phase is examples of one-dimensional continuity, the lamellar phase of two continuity, while three-dimensional continuity is found for the bicontinuous cubic phase, for the sponge phase [2]. Phase structures of surfactant micelles altered with the architecture of the surfactant.

Holmberg et al. [3] related the head group area, the extended length and the volume of the hydrophobic part of a surfactant molecule in to a dimensionless number, critical packing parameter (CPP$=\nu/(l_{\max}a)$). The geometry of the micelle was found to be determined by different CPP values. Holmberg et al. proposed the concept of CPP by characterizing the micelle core as a hydrocarbon droplet with a radius equalizing the length of the extended alkyl chain of the surfactant. The aggregation number (N) can be expressed as the ratio between the micellar core volume (V_{mic}) and the volume (ν) of one-chain.

$$N = \frac{V_{\text{mic}}}{\nu} = \frac{(4/3)\pi R_{\text{mic}}^3}{\nu}$$

The aggregation number (N) can alternatively be expressed as the ratio between the micellar area (A_{mic}) and the cross-sectional area (a) of one surfactant molecule.

$$N = \frac{A_{\text{mic}}}{a} = \frac{4\pi R_{\text{mic}}^2}{a}$$

Putting these aggregation numbers as equal, the correlation was derived as follows:

$$\frac{\nu}{R_{\text{mic}}a} = \frac{1}{3}$$

Since R_{mic} cannot exceed the extended length of the surfactant alkyl chain ($l_{\max}$), Holmberg et al. found that for $\nu/(l_{\max}a) \leq 1/3$, the critical packing shape is a cone with base area a. Self-assembly of such cones generally leads to spherical micelle structure. Highly truncated cones are obtained as $(1/2) < \text{CPP} < 1$, where self-assembly of such cones leads to bilayers such as found in vesicles and liposomes. In this study,

* Corresponding author. Tel.: +886 4 24517250x3678; fax: +886 4 24510890.
E-mail address: changcj@fcu.edu.tw (C.-J. Chang).

0032-3861/$ - see front matter © 2005 Elsevier Ltd. All rights reserved.
doi:10.1016/j.polymer.2005.11.075

CPP is used to discuss the type of structure formed by the branched reactive surfactant.

Much work has been devoted to the variation of the nature of the emulsifier, which is normally a low molar mass surfactant. The use of polymerizable surfactants has been studied [4–15]. These reactive surfactants can copolymerize with the main monomer and become covalently bound to form an integral polymeric material. Migration in the polymer film is impeded. Such improvements of latex and polymer properties have been reported for mechanical stability [6], electrolyte stability of the latex [7], control of surface charge density [16], and a decrease of surfactant migration [17]. Bucsi et al. [18] devoted to the functionalization of PS latexes by linear PEO-*b*-PS based macromonomers. Zana et al. [19] reported the synthesis and the use of ionic surfmers that exhibit a gemini structure in emulsion polymerization. Heroguez et al. [20] reported nonionic PS-*b*-PEO_2 gemini-type dispersants made by a multiple-step synthesis.

The paper mainly focuses on the synthesis of comb-type branched emulsifiers that is curable, self-assemble and investigating the influence of the molecular architecture of emulsifiers on the outcome of polymerization. The comb emulsifier synthesized in this study can be viewed as a surfactant trimer with the heads bounded together. The fact that dimeric or gemini-type surfactants exhibit better wetting, foaming and dispersing performances than conventional surfactants [21] prompted us to examine the potential of comb surfactant as reactive emulsifiers. Two molecular architectures of comb-like emulsifiers were studied, which should give rise to different behavior. We were interested to learn about the ability of comb-like polymerizable surfactants to function as emulsifier in emulsion polymerization. As such systems depend on numerous parameters which render an absolute evaluation difficult, the polymerization of styrene emulsion and copolymerization of styrene and butyl acrylate were studied for these polymerizable surfactants. These surfactants are characterized by an increasing content of hydrophobic chains. The EO segment is needed to assure the water solubility of the comb dispersants. The hydrophobe content was controlled under the maximum which still allows solubility of such head-type emulsifiers in water. This contribution is more specifically devoted to their use in the preparation of interconnected multi-lamellar particles. The polymerizable comb architecture may provide possibility of altering shape of the latex particles.

In this study, the feasibility of polymerizable comb-like branched surfactants with different hydrophobic chains and unsaturated methacryloyl moieties to act as emulsifier in emulsion polymerization, together with the correlation between the particle shape and the emulsifier structure were investigated.

2. Experimentals

2.1. Materials

The monomers including *n*-butyl acrylate (Lancaster), styrene(Acros), glycidyl methacrylate(TCI), acrylic acid (WAKO) were distilled in a vacuum before use. The initiator, potassium persulfate (KPS, Acros Organics), was of the analytical grade and used as received. Hydroquinone (Showa) was used without purification. DMF was stirred over $MgSO_4$ and then vacuum distilled. Succinic anhydride (SA) and l,2,4-benzenetricarboxylic anhydride (BTCA) were supplied by Aldrich Co. Polyoxyethylene(26) glycerol was supplied by Lipo Co.

2.2. Synthesis of polymerizable emulsifier

Comb-like UV curable emulsifier (G26BG) was synthesized from polyoxyethylene(26) glycerol as the core molecule (GEO26), 1,2,4-benzenetricarboxylic anhydride (BTCA) as an AB2 monomer, and glycidyl methacrylate (GMA) as an endgroup modifier. Ideally, G26BG has six methacryloyl moieties (six arms). Less branched emulsifier G26SG was synthesized by substituting succinic anhydride (SA) for BTCA. Ideally, G26SG has three methacryloyl moieties (three arms). There are methacryloyl moieties at each terminal group of the side-chain. These hydrophobic segments are attached to the hydrophilic comb-segments. The surfactants are characterized by an increasing content of hydrophobic chains and increasing unsaturated methacryloyl moieties.

The polymerizable emulsifiers were synthesized by the following two-step routes that afforded samples of precisely controlled functionality and size.

2.3. Synthesis of G26BG

Polyoxyethylene(26) glycerol (2.04 g) was dissolved in DMF (9 g) in a three-necked flask. Then BTCA (0.95 g) was added into the flask. The flask was moved to an oil bath at 90 °C and stirred by a magnetic bar. The mixture was left to react for 8 h under nitrogen atmosphere. The extent of reaction was monitored by the FTIR spectra of the reaction mixture. The absorption peak at 1850 cm^{-1} (carbonyl group of BTCA) was disappeared after reacting for 8 h.

The heating temperature of the reaction mixture was kept at 70 °C. GMA (1.41 g) was dissolved in DMF (4.5 g) and then poured into the above mixture and reacted for 8 h under nitrogen atmosphere. The extent of reaction was monitored by the FTIR spectra of the reaction mixture. The absorption peak at 908 cm^{-1} (oxirane ring of GMA) was disappeared after reacting for 8 h. The solution was first vacuum dried. The baking temperature was set at 30 °C for 30 min, and then raised to 50 °C for 30 min and 70 °C for 30 min. The dried compound was washed with methanol. The purified sample was used for the characterization by NMR and as emulsifier for the following emulsion polymerization. The reaction scheme is shown in Scheme 1.

^{1}H NMR (δ, ppm, *d*-DMSO): l.95 (18H, 6 segments of –$COC(CH_3)CH_2$); 3.1–3.7 (109H, $CH_2(EO)_xCH(EO)_yCH_2(EO)_z$, and 26 repeating units of –OCH_2 CH_2O–); 3.7–4.3 (24H, 6 segments of –$COOCH_2CH(OH)CH_2O$–); 4.3–4.7 (6H, 6 segments of –$COOCH_2CH(OH)CH_2O$–); 5.6–6.1 (12H, 6 segments of –$COC(CH_3)CH_2$); 7.6–8.2 (9H, Ar*H*).

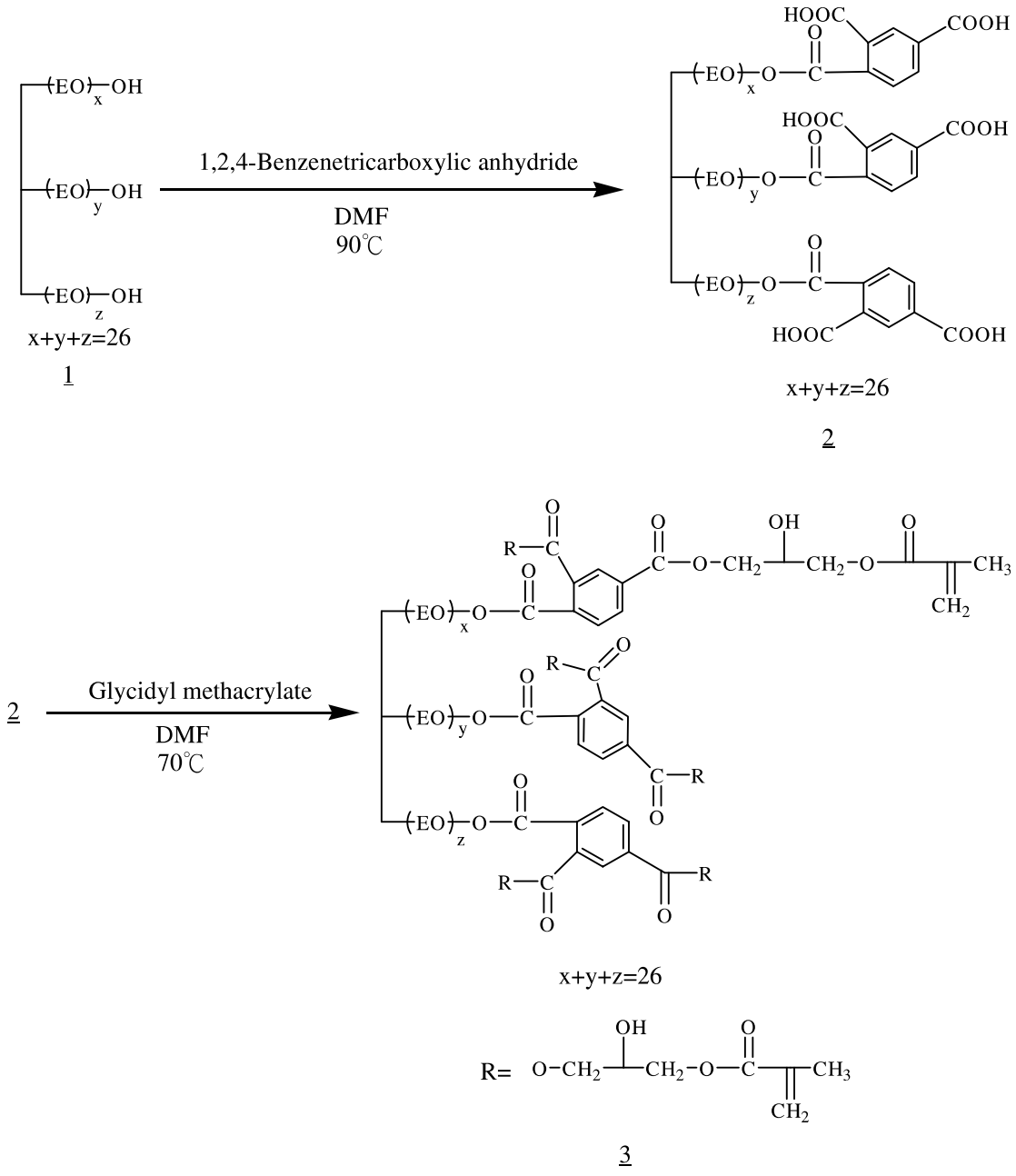

Scheme 1. Synthesis route of the G26BG emulsifier.

2.4. Synthesis of G26SG

Polyoxyethylene(26) glycerol (2.04 g) was dissolved in DMF (9 g) in a three-necked flask. Then SA (0.58 g) was added into the flask. The flask was moved to an oil bath at 90 °C and stirred by a magnetic bar. The mixture was left to react for 8 h under nitrogen atmosphere. The extent of reaction was monitored by the FTIR spectra of the reaction mixture. The absorption peak at 1786 cm^{-1} (carbonyl group of SA) was disappeared after reacting for 8 h.

The heating temperature of the reaction mixture was kept at 70 °C. GMA (0.83 g) was dissolved in DMF (2.5 g) and then poured into the above mixture and reacted at 70 °C for 8 h under nitrogen atmosphere. The extent of reaction was monitored by the FTIR spectra of the reaction mixture. The absorption peak at 908 cm^{-1} (oxirane ring of GMA) was disappeared after reacting for 8 h. The solution was vacuum dried. The baking temperature was set at 30 °C for 30 min, and then raised to 50 °C for 30 min and 70 °C for 30 min. The dried compound was washed with methanol. The purified sample was used for the characterization by NMR and as emulsifier for the following emulsion polymerization. The reaction scheme is shown in Scheme 2.

^{1}H NMR (δ, ppm, *d*-DMSO): 1.95 (9H, 3 segments of –COC(CH_3)CH_2); 2.5–2.7 (12H, 3 segments of –OOCCH_2CH_2-COO–); 3.1–3.7 (109H, CH_2(EO)$_x$CH(EO)$_y$$CH_2(EO)_z$, and 26 repeating units of –OCH_2 CH_2O–); 3.7–4.3 (15H, 3 segments of –COOCH_2CH(OH)CH_2O–); 5.6–6.1 (6H, 3 segments of –COC(CH_3)CH_2).

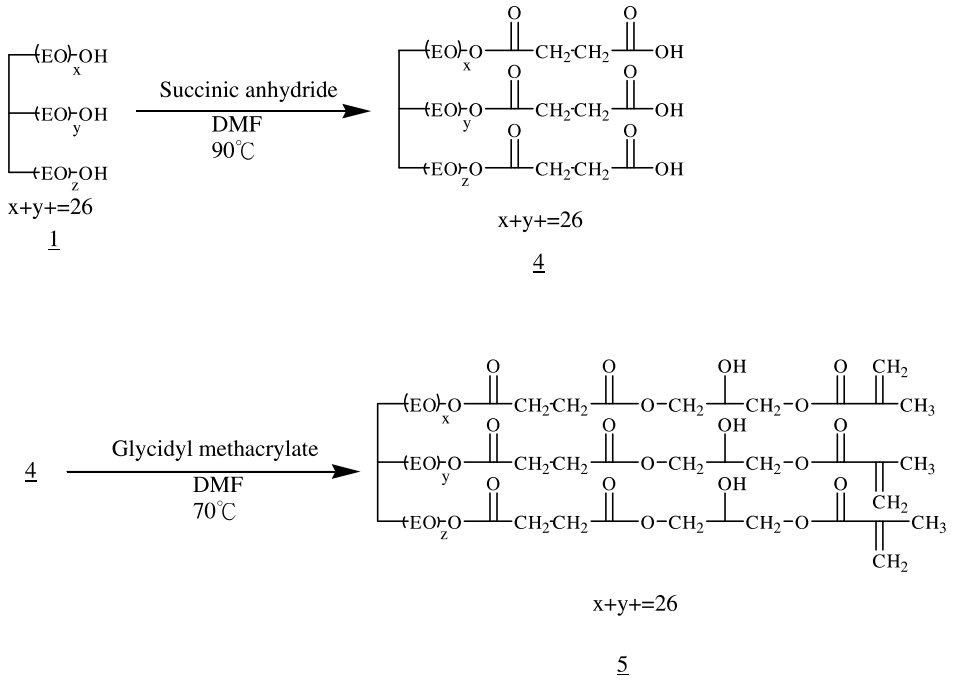

Scheme 2. Synthesis route of the G26SG emulsifier.

2.5. Emulsion polymerization

Emulsion polymerizations were carried out in a 100 mL three-neck glass reactor equipped with stirrer, nitrogen inlet and reflux condenser with the recipes listed in Table 1. The stirring speed was 200 rpm.

Two types of reference experiments were performed for comparison. The experimental procedure was as follows: the seed and a fraction of water, G26BG and KPS were initially charged into the reactor. The rest was fed in two streams having the same feeding time. One of the streams was a pre-emulsion of the monomer mixture and the other an aqueous solution of the initiator.

The compositions were fed in two streams having the same feeding time. One of the streams was the monomer mixture and the other was an aqueous solution of the initiator. A typical composition of 0.09 g of G26BG, and 25 g of water was added into a flask with stirring and nitrogen bubbling for 10 min an initiator consisting of 0.045 g of KPS in 5 g of water was then introduced into the emulsion at 70 °C. 0.8 g of BA, 0.8 g of ST, 0.09 g of AA, 0.09 g of GMA monomers were added dropwise to the emulsion. During the addition of monomers, nitrogen was continuously bubbled into the system with the stirring at about 200 rpm.

2.6. Characterization

Scanning electron microscopy analysis (SEM) was performed with a HITACHI S3000 variable vacuum scanning electron microscope and energy-dispersive spectrometer. A syringe was used to withdraw 2.5 mL of the polymerized emulsion through a rubber septum at different polymerization intervals. A small amount (0.4 mL) of hydroquinone (3% solution) was mixed with each drawn sample to terminate the polymerization. The latex sample was diluted and used for the observation of the morphology by SEM. One drop of the colloidal dispersion was put on a glass and allowed to air-dry before observation.

Transmission FTIR spectra were collected on the Shimadzu IR Prestige-21 spectrometer.

^{1}H NMR spectra were performed using a Varian Inova 600 high field nuclear magnetic resonance spectrometer.

Measurements of the surface tension were carried using a Kruss K6 tensiometer. Critical micellar concentrations were determined by looking for the discontinuity on the log (concentration) vs. surface tension curve. A stock solution was first prepared. Then, a series of solutions with different concentrations were prepared by successive dilution of the stock solution. Surface tension measurement was recorded for several times to ensure an internal reproducibility for each solution.

DSC was carried out using a MDSC 2920 apparatus from TA Instruments at a scan rate of 10 °C/min for both heating and

Table 1
Recipes of the latex solution for emulsion polymerization

	EM1 (g)	EM2 (g)	EM3 (g)	EM4 (g)
G26BG	0.09		0.09	
G26SG		0.09		0.09
KPS ($K_2S_2O_8$)	0.045	0.045	0.045	0.045
Water	30	30	30	30
Styrene	0.8	0.8	1.6	1.6
Butyl acrylate	0.8	0.8		
Acrylic acid	0.09	0.09	0.09	0.09
Glycidyl methacrylate	0.09	0.09	0.09	0.09

cooling. The reported glass transition temperatures were determined from the second heating run.

The overall conversion of the polymerization vs. the time was determined upon gravimetry determination of the weight of the polymer formed after a given time.

3. Results and discussion

The CMCs of the surfactants were determined by surface tension measurements. The surface activity of these surfactants is shown in Fig. 1. The lowering of the water surface tension and the micelle formation clearly revealed the amphiphilic character of both synthesized molecules. Hence a surfactant character was proven for both new compounds. When comparing the surface activity of the two compounds, significant differences were observed depending on the type of branched surfactants used. Although the two surfactants exhibit the same number of ethylene oxide repeating units, aromatic branched emulsifier (G26BG) had bulky hydrophobic aromatic ring and more branched side-chains than the aliphatic compound (G26SG) did. There are six and three unsaturated branched side-chains (methacryloyl moieties) for G26BG and G26SG respectively. The critical micelle concentration (CMC) value on aromatic branched emulsifier (G26BG) is slightly lower than the one measured for the aliphatic branched emulsifier (G26SG).

Surfactant micelles can be used as building blocks to form different phase structures in solution such as spherical, prolate, oblate, cylindrical, hexagonal and lamellar phase. In addition to spherical particles, this article is the first study to prepare lamellar particles by emulsion polymerization using suitable UV curable comb-like branched surfactants. UV curable comb-like branched surfactants with different extended length, the volume and functionality of the hydrophobic part and suitable monomer helped the formation of lamellar structure. The polymerizable emulsifiers were immobilized on the latex particles and improved the latexes' stability. It facilitated the formation of lamellar and spherical particles. This study provided a new approach to prepare lamellar particles and

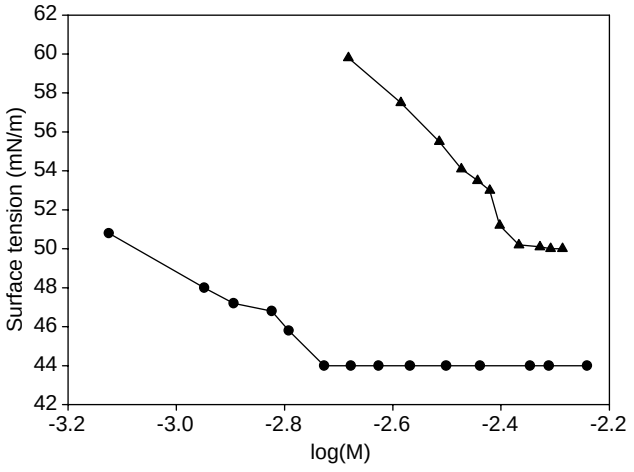

Fig. 1. Surface tension of the G26BG (●) and G26SG (▲) emulsifiers at different concentrations.

illustrated the correlation between the particle shape and surfactant structure. For the traditional single-chain surfactant, the lamellar phase was usually found at a higher concentration. G26BG and G26SG surfactants had six and three unsaturated branched side-chains (methacryloyl moieties) respectively. Comb-like branched structures of G26BG and G26SG surfactants with high methacryloyl-moieties structures helped the formation of lamellar structures at lower concentration. When the content of these surfactants with high methacryloyl-moieties structures increased, the medium began to coagulate at the early stage of the emulsion polymerization process. Suitable reaction condition helped to immobilize the polymerizable emulsifier on the latex particles. Higher content will lead to unexpected coagulation. It is the major difference between reactive comb-like branched surfactant and traditional single-chain surfactant. In this study, according to recipes listed in Table 1, the amount of comb-like branched G26BG and G26SG surfactants were kept low to prevent unexpected coagulation.

The SEM micrographs of particles formed at different periods of the emulsion polymerization were shown in Fig. 2. Fig. 2(a) and (b) is the SEM micrographs of particles formed at 60 min. As shown in Fig. 2(a), sword-like latex particles were observed. A single octagonal planar particle was shown in Fig. 2(b). Fig. 2(c) exhibited the SEM micrographs of particles formed at 120 min. The planar particles and sword like particles were the majority of the particles. The planar particles were slightly larger than that observed at 60 min as shown in Fig. 2(b). G26BG was a triple-chain surfactant with relative large head group and large branched tail. Such molecular structure favored the self-assembling of layered architecture. The lamellar phase was formed by extended regions of surfactant double layers. Fig. 2(d) exhibited the SEM micrographs of particles formed at 140 min. The image was similar to Fig. 2(c) except some stacked planar particles were observed. The enlarged images of the stacked planar particles were shown in Fig. 2(e). Single planar and sword-like particles were still the dominant microstructures. The amount of stacked planar particles was less than that of single planar particles. The single and stacked planar particles were the majority.

We made two comparative experiments to check whether the planar particles were crystals of hydroquinone (HQ) or KPS. In the first test, 0.045 g of KPS was dissolved in 32 g D.I. water. In the second experiment, 0.4 mL hydroquinone (3% solution) was mixed with 2.5 mL D.I. water. Both aqueous solutions were heated to 70 °C and then cooled to room temperature. One drop of each solution was put on a glass and allowed to air-dry before SEM observation. SEM images of KPS and HQ particles derived from drying of dilute aqueous KPS and HQ solution were illustrated in Fig. 3(a) and (b), respectively. Fig. 3(a) showed that the shape of KPS particle was more irregular than those of the latex particles shown in Fig. 2. Fig. 3(b) showed that the HQ particle was not planar particle. We excluded the possibility that the planar particles were the crystal of HQ.

In order to confirm that the planar particles was the G26BG//ST/BA latex particles, qualitative identification of the

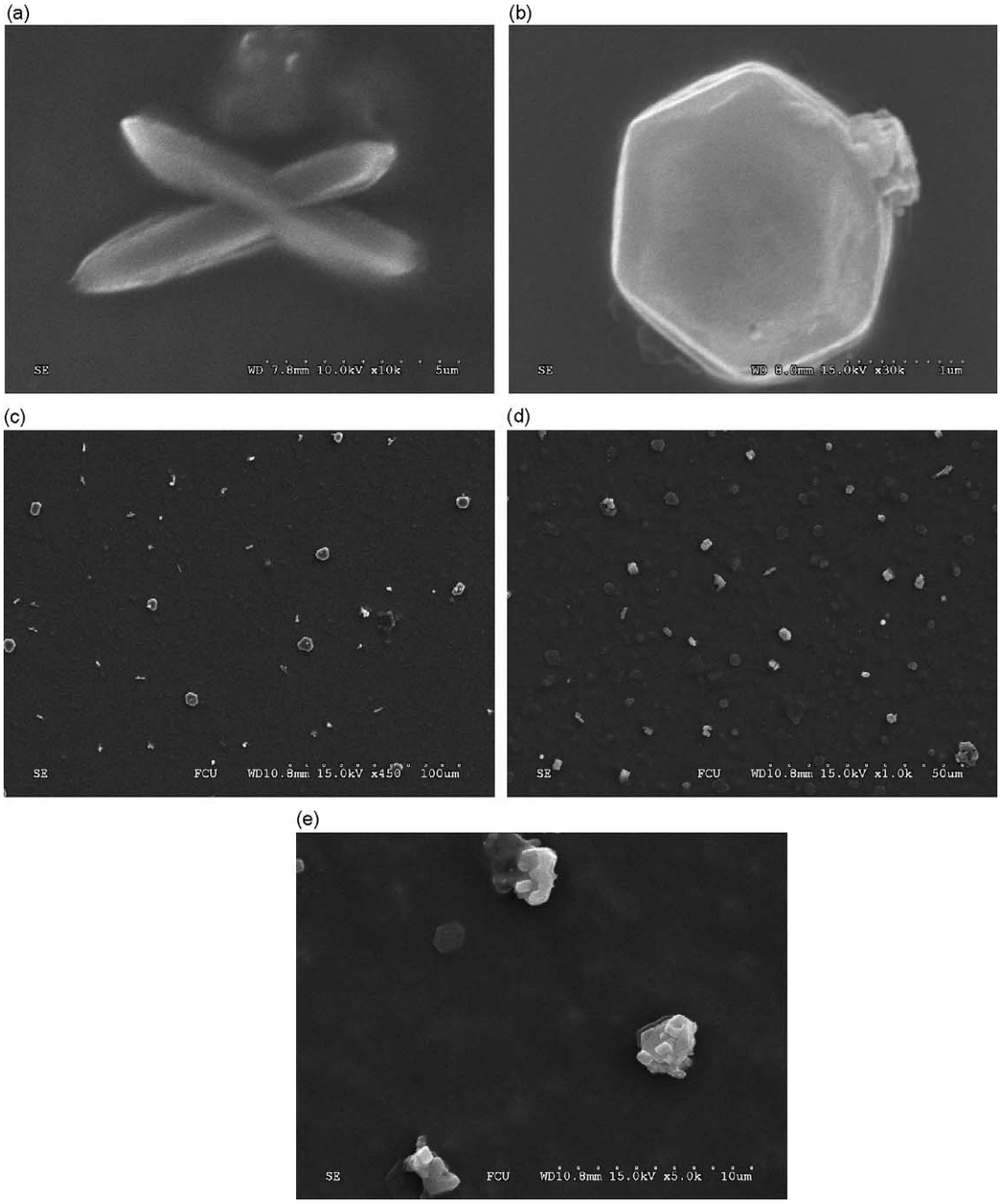

Fig. 2. SEM images of the (a) sword-like latex particles (b) octagonal planar latex particle formed at 60 min (c) planar particles formed at 120 min (d) planar particles formed at 140 min (e) enlarged images of stacked planar particles using G26BG emulsifier, styrene and butyl acrylate monomers.

glass substrate, G26BG//ST/BA latex polymeric particles (the sample shown in Fig. 2(c)) and KPS particles (the sample shown in Fig. 3(a)) were done by energy-dispersive X-ray (EDX) spectrometry. The results were illustrated in Fig. 4(a)–(c), respectively. The calculated element content was listed in Table 2. The Si element came from the glass substrate. The C element mainly came from the G26BG emulsifier, styrene and the acrylate monomers. KPS was the major source of K and S elements. There were several possible sources of O element. The glass substrate, the G26BG emulsifier, the acrylate monomers and initiator KPS contained the O element. Analyzing relative content of C, K and S elements helped to distinguish whether the planar particles was the latex particle or the crystal of initiator KPS. Although small amount of KPS initiator might be incorporated in the latex polymeric particle during the emulsion polymerization reaction, the KPS crystal should have higher content of K and S elements than the latex particle did. Fig. 4(a) showed that the glass substrate had large amount of Si and O elements. Fig. 4(b) revealed that the G26BG//ST/BA latex polymeric particles contained large amount of C element (at.% = 34.58%). The EDX spectrometry of the KPS crystal in Fig. 4(c) showed large amount of K and S elements (K at.% = 18.44%, S at.% = 12.85%) than those of the G26BG//ST/BA latex polymeric particles in Fig. 4(b) (K

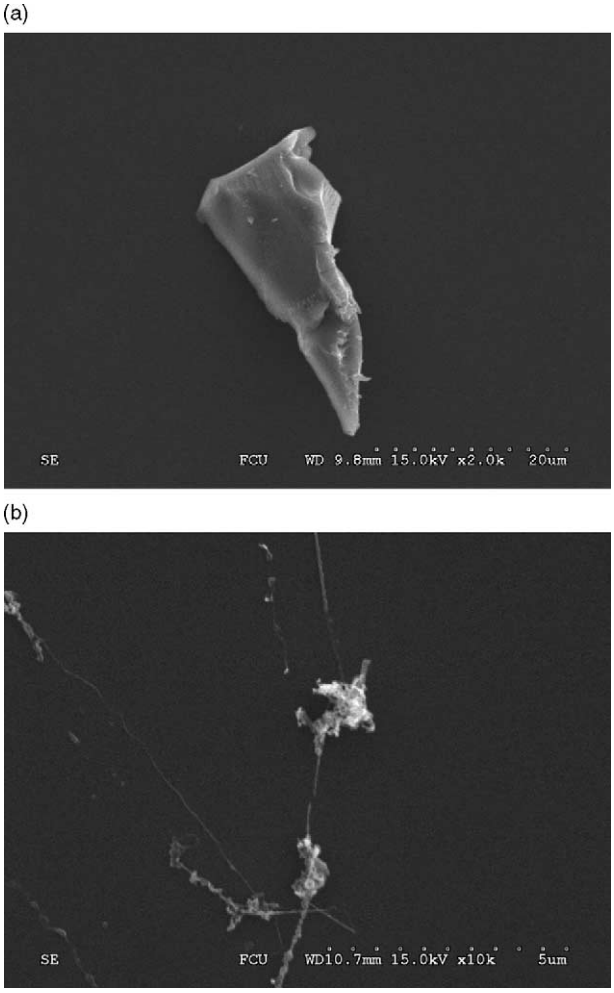

Fig. 3. SEM images of (a) KPS (b) HQ particles derived from drying of dilute aqueous KPS and HQ solution.

at.%=4.80%, S at.%=2.50%). The C element content of the KPS crystal in Fig. 4(c) was about the same as that of the glass substrate in Fig. 4(a). These results revealed that the planar particles shown in Fig. 2(c) were different from the KPS particles shown in Fig. 3(a). The planar particles shown in Fig. 2(c) were the G26BG//ST/BA latex polymeric particles.

A less branched emulsifier G26SG with smaller aliphatic tail was used for comparison. The SEM micrograph of the latex particles using G26SG emulsifier, styrene (ST) monomer and butyl acrylate (BA) monomers according the EM2 recipes of Table 1 was shown in Fig. 5. It presented the oblate latex particles.

Copolymer G26SG//ST/BA (Fig. 6(a)) exhibited a T_g at 10 °C. The DSC spectrum of copolymer G26BG//ST/BA (Fig. 6(b)) shows two T_g. The first one is under room temperature (10 °C) and is currently more intensive; the second one of less intensity is above room temperature (30 °C). Polymerizable emulsifiers can copolymerize with the main monomer and become covalently bound to form an integral polymeric material. G26BG and G26SG emulsifiers had six and three unsaturated branched side-chains (methacryloyl moieties) respectively. Both emulsifiers can also act as

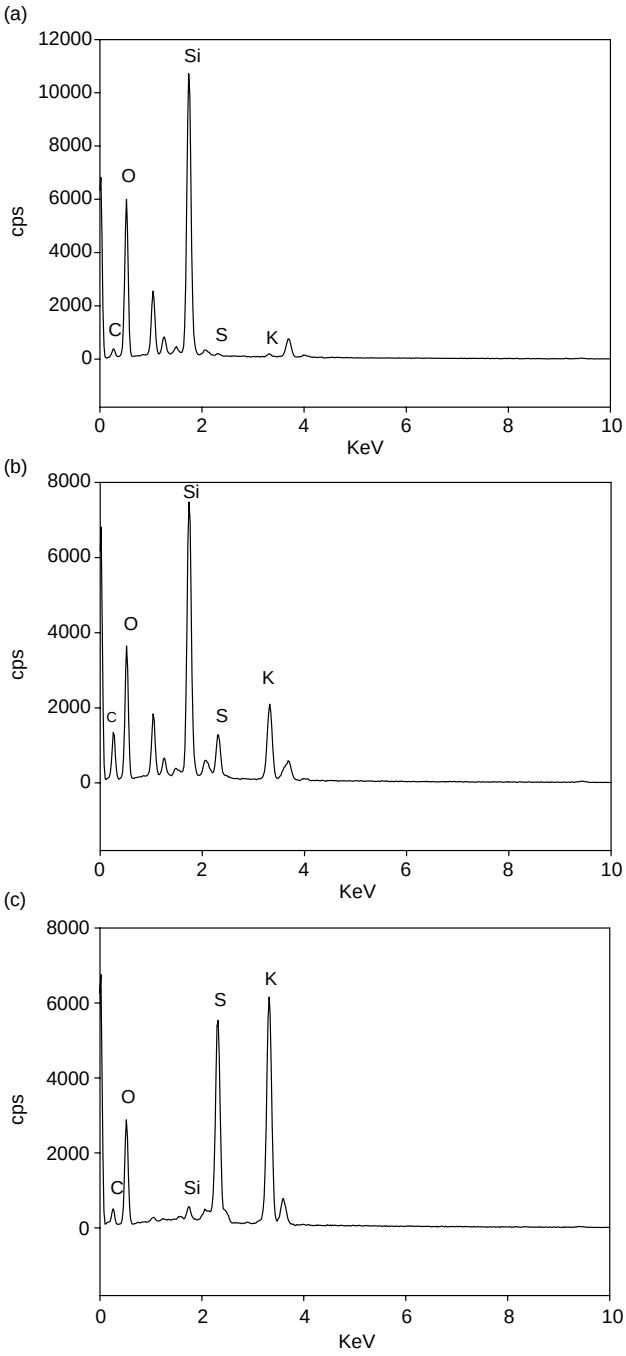

Fig. 4. Energy-dispersive X-ray spectrometry of (a) the glass substrate (b) the latex particle prepared by using G26BG emulsifier, styrene and butyl acrylate monomers (c) the KPS particle derived from drying of dilute aqueous KPS solution.

crosslinker once more than two methacryloyl moieties on the same molecule polymerized with adjacent monomers or emulsifiers. Since G26BG or G26SG was the only emulsifier used in this recipe, most of the emulsifiers located at the outer shell boundary of the micellar layers. The effect of crosslinking had more influences on the properties of the particle shell than those of the particle core. G26BG had more unsaturated branched methacryloyl moieties than G26SG. In addition, the G26BG molecule contained aromatic ring while G26SG had

Table 2
The major element contents of different samples measured from the energy-dispersive X-ray (EDX) spectrometry

Sample element	Glass substrate		G26BG//ST/BA		KPS	
	wt%	at.%	wt%	at.%	wt%	at.%
C	9.01	14.14	23.09	34.58	7.57	13.80
O	46.29	54.80	36.31	40.84	37.23	52.92
Si	33.28	22.33	19.64	12.58	1.00	0.78
S	0.45	0.27	4.46	2.50	18.81	12.85
K	0.64	0.31	10.43	4.80	32.92	18.44
Na	7.56	7.56	5.59	4.37	0.47	0.45

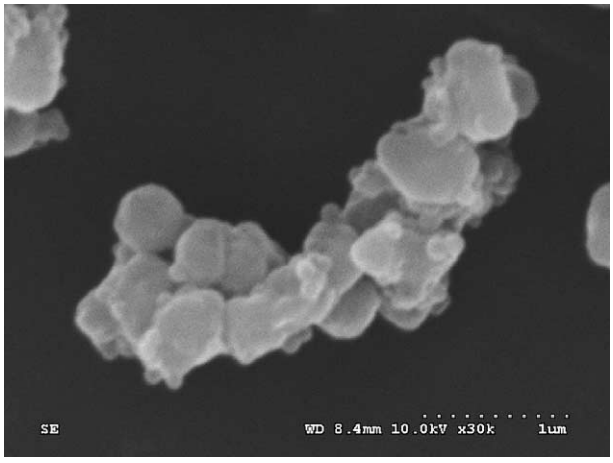

Fig. 5. SEM images of the oblate latex particles using G26SG emulsifier, styrene and butyl acrylate monomers formed at 240 minutes.

only aliphatic chain. For G26BG//ST/BA, an additional transition above room temperature (30 °C) was observed and might be attributed to the effect of crosslinking of the G26BG. Laruelle et al. [22] performed the DSC tests on homopolymer PS and homopolymers PBA of different molar mass. T_g of free PBA was comprised between −53 °C for smaller molecular weight PBA (M_n = 25,000 g/mol) and −47 °C for larger molecular weight PBA (M_n = 13,0000 g/mol) respectively. T_g of PS (with the M_n = 10,000 g/mol) is 97 °C. T_g of the PS is very high in comparison with PBA so when the glass transition of the PBA occurs, the G26BG//ST/BA polymer chain are fixed by two factors, one by the rigidity of the PS the other by the crosslinking. Then the motion of the PBA segment is hindered

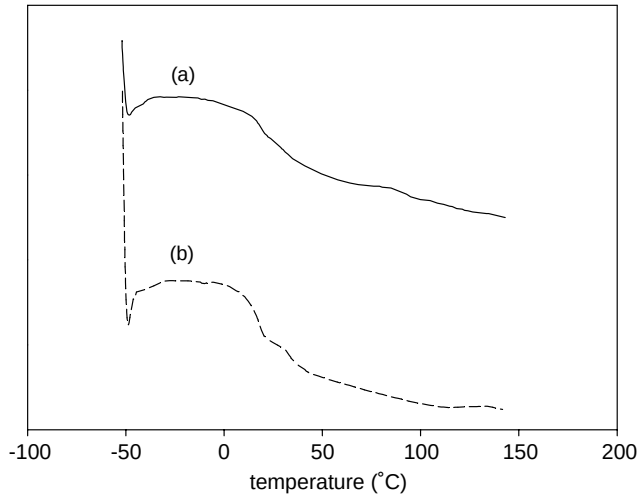

Fig. 6. DSC thermograms of (a) polymers prepared by using styrene and butyl acrylate monomers and (a) G26SG emulsifier (b) G26BG emulsifier.

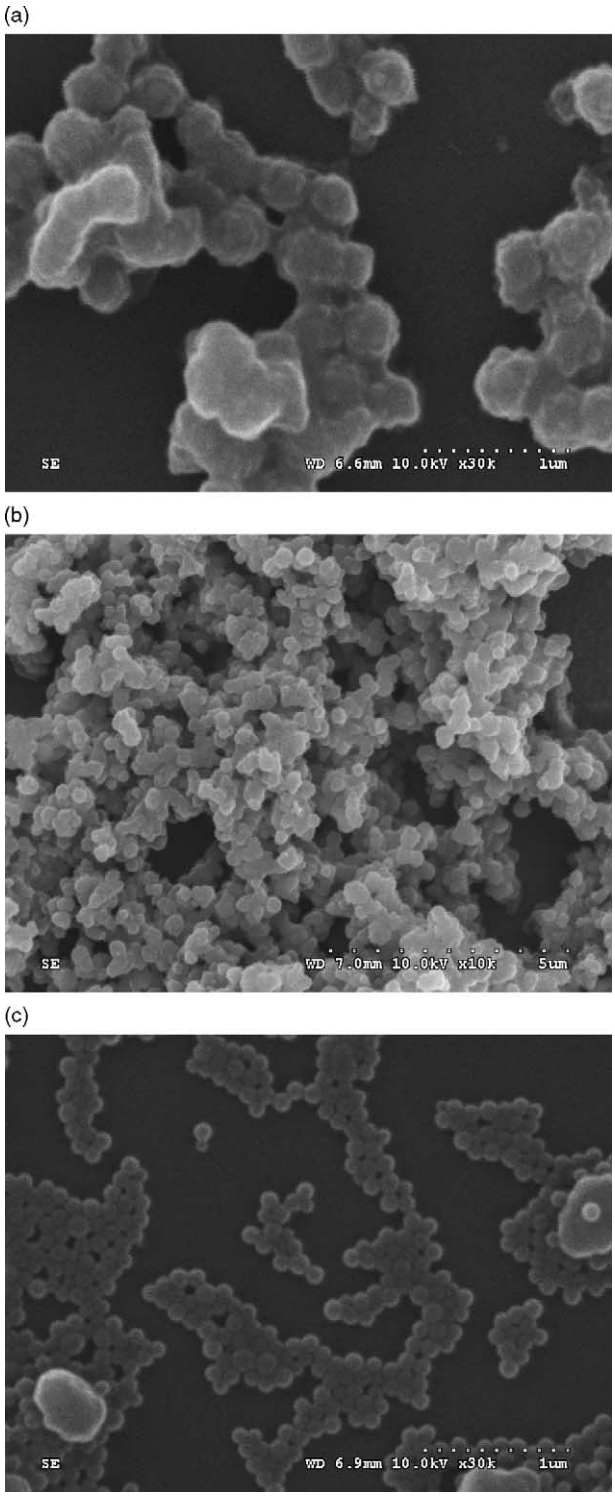

Fig. 7. SEM images of the oblate latex particles formed at (a) 180 min (b) 240 min using G26BG emulsifier and styrene monomer (c) the spherical latex particles using G26SG emulsifier and styrene monomer formed at 240 minutes.

and more energy is needed to pass from a glassy slate to a rubbery state, thereby increasing the temperature of the glass transition of the polymer. The higher temperature transition above room temperature (30 °C) is of less intensity because the amount of emulsifiers is much less than the monomers and the crosslinking is more likely to occur near the outer shell, rather than the whole latex particles. In the SEM observation experiments in Figs. 2 and 5, latex dispersion was put on a glass and allowed to air-dry at 22 °C. The G26SG//ST/BA latex particles had T_g at 10 °C. Deformation during the drying process may have some influences on the shape of the G26SG//ST/BA particles (shown in Fig. 5). But deformation during drying had less influence on the shape of the G26BG//ST/BA particles (shown in Fig. 2).

Fig. 7(a) and (b) illustrated the SEM images of the latex particles formed at 180 and 240 min using G26BG emulsifier and styrene monomer according the EM3 recipes of Table 1. The conditions were the same as those shown in Fig. 2 except the monomer. Different shape of latex particles was observed. The oblate shape rather than the planar structure was derived and shown in Fig. 2. It showed short ranged planar-like structure but with macroscopic spherical architecture with poor circularity. A less branched emulsifier G26SG with smaller aliphatic tail was used for comparison. The SEM micrographs of the latex particles using G26SG emulsifier, styrene (ST) monomer according the EM4 recipes of Table 1 were shown in Fig. 7(c). The reaction conditions were the same as those shown in Fig. 4 except the monomer. It showed spherical latex particles with good circularity.

The extended length and the volume of the hydrophobic part of a surfactant molecule were related in to a dimensionless number CPP. The ratio $v/(l_{max}a)$, denoted as the critical packing parameter (CPP), gives a geometric characterization of a surfactant molecule. Holmberg et al. [3] found that for

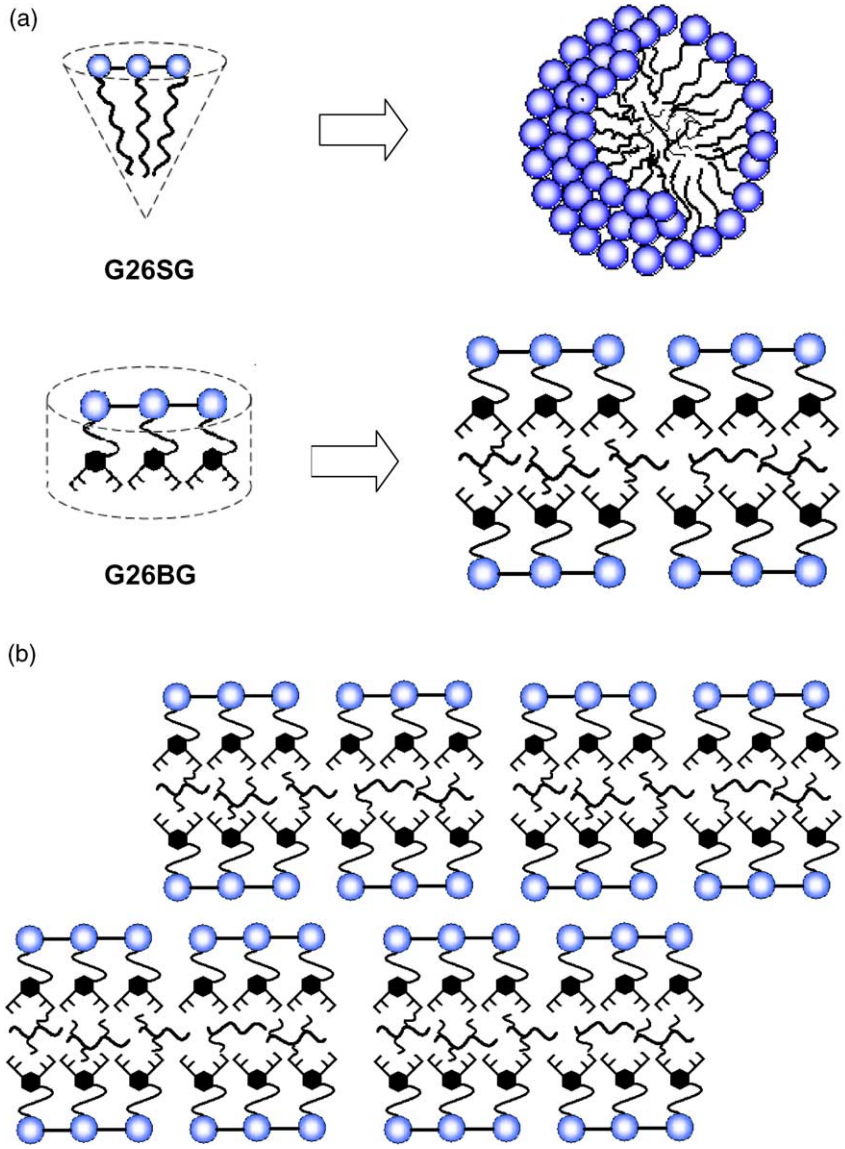

Fig. 8. Schematic illustration of (a) emulsifiers with different head/tail size and preferred latex particle shape for geometrical packing reason (b) formation of stacked planar particles.

CPP ≤ 1/3, the critical packing shape is a cone with base area *a*. Self-assembly of such cones generally leads to spherical micelle structure. Highly truncated cones are obtained as (1/2) < CPP < 1, where self-assembly of such cones leads to flexible bilayers such as found in vesicles and liposomes. In this study, CPP is used to discuss the type of structure formed by the branched reactive surfactant. We proposed that similar explanation was also valid for the emulsion polymerization using emulsifiers with different geometry, as shown in Fig. 8(a). The coil conformation of G26SG and G26BG molecules are more like cones and highly truncated cones (or cylinder) respectively. G26SG favored the formation of spherical or oblate microstructure. G26BG favored the formation of planar (lamellar) microstructure. Fig. 8(b) illustrated the formation of stacked planar particles. The planar particles had the chance to get closer when the concentration of planar particles became higher. The stacked planar particles formed after the evaporation of the water between two adjacent particles.

Fig. 9(a) presented the overall conversion for the emulsion polymerization of styrene monomer using G26BG and G26SG emulsifiers at different periods of the emulsion polymerization.

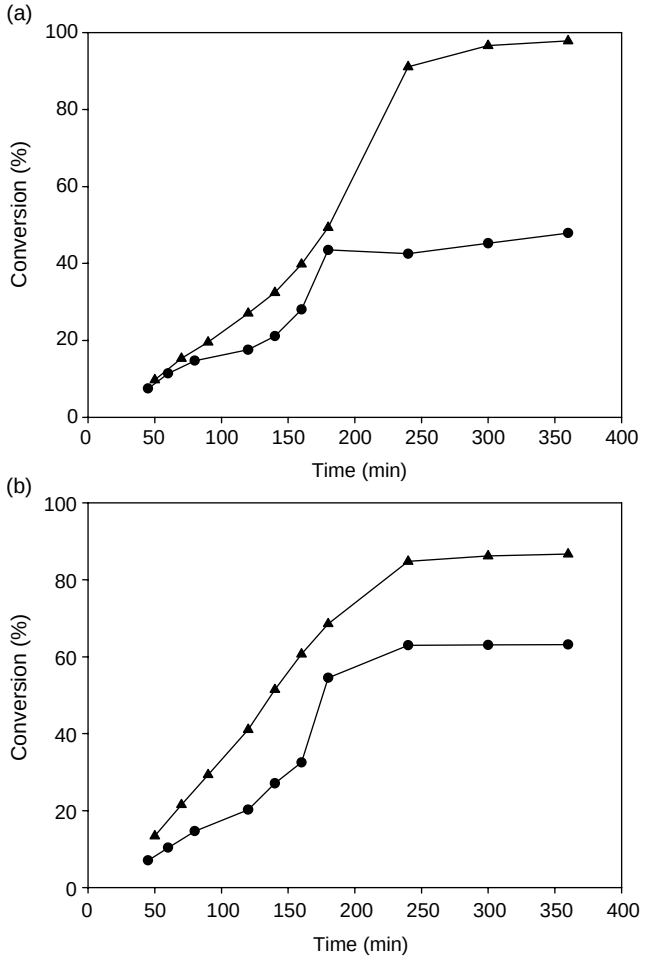

Fig. 9. Overall conversion for the emulsion polymerization of (a) styrene monomer (b) styrene and butyl acrylate monomers using G26BG (●) and G26SG (▲) emulsifiers at different time.

For G26BG emulsifier and styrene monomer with the EM3 recipe, the final conversion was close to 50%, lower than that of G26SG (>95%) using the EM4 recipe. Besides, the conversion curve exhibited a slow increase and saturated soon for the G26BG surfactant. The mechanism of particle nucleation in emulsion polymerization is described as proceeding by two simultaneous processes, micellar nucleation and homogeneous nucleation. Micellar nucleation is the entry of radicals (primary radicals and oligomeric radicals) from the aqueous phase into the micelles. Homogeneous nucleation involves the solution-polymerized oligomeric radicals becoming insoluble and precipitating on themselves. The precipitated species become stabilized by absorbing emulsifiers from solution and monomer droplets. Highly water soluble monomers favored homogeneous nucleation, while water insoluble monomers favored micellar nucleation. Since styrene and butyl acrylate are relatively water insoluble monomers, micellar nucleation is the predominant mechanism in this study. Emulsifiers serve four main functions in the micellar-nucleation dominant emulsion polymerization. The first is to provide surface absorption and temporary emulsion droplet stabilization of monomer droplets in the two phase reaction mixture. Modest shear enables the monomer to be dispersed as crude emulsion. These droplets constitute reservoirs of monomer and are depleted as polymerization proceeds. The second is to provide a site for the formation of small oligomers as polymerization is initiated. Emulsifier micelles provide such sites by offering a region of intermediate solubility to the bulk monomer phase in the emulsion droplets and the bulk aqueous phase. Another function is facilitating transport between the monomer emulsion droplet and the reacting, polymerizing polymer (the radicals, or oligo-radicals). The fourth function is to stabilize the polymer particles as they grow in size during polymerization. The emulsifier used in this study can be considered as the surfactant trimer which has three hydrophilic/hydrophobic chains connected at the hydrophilic end. The chemical structure of the emulsifier such as the volume of the polymerizable tail was adjusted and exhibited great influence on the function of the emulsifiers.

G26BG has bulky hydrophobic tails. Meanwhile, styrene also has a bulky phenyl side group. The slow increase of conversion curve for G26BG was due to two reasons. The first was the difficulty for the styrene monomer, the primary radicals and oligo-radicals to diffuse inside the reacting, polymerizing polymer micelle because of steric hindrance. Besides, there might be copolymerization between the polymerizable emulsifier and radicals (or oligo-radicals) during the diffusion process. The polymerization may form a shell around the reacting micelle. The shell acted as the diffusion barrier and hindered the transport of monomers and the radicals (or oligo-radicals). G26BG has more methacryloyl moieties and is more reactive toward the transporting radicals (or oligo-radicals) than G26SG does. The diffusion barrier around the reacting micelle of G26BG based emulsion polymerization formed easier and faster than that of G26SG based emulsion polymerization. Once the barrier can block the transportation of monomer and the radicals (or oligo-radicals), the emulsion

polymerization stopped. The conversion will not increase anymore. That may explain why the final conversion of G26BG was lower than that of G26SG and the conversion curve of G26BG exhibited a fast saturation.

Fig. 9(b) presented the overall conversion for the emulsion polymerization of styrene and butyl acrylate monomers using G26BG and G26SG emulsifiers at different periods of the emulsion polymerization. Comparing Fig. 9(b) with (a), the conversion curve for ST/BA monomers was about the same as that of ST monomer using G26SG emulsifier. However, the final conversion for ST/BA monomers was higher than that of ST monomer using G26BG emulsifier. Since BA monomer is smaller than ST monomer. It helped the entry of radicals from the aqueous phase into the micelles. An increase in the conversion curve using G26BG emulsifier was observed in Fig. 9(b). The polymerization conversion depends on the molecular architectures of the emulsifiers and monomers.

4. Conclusion

In addition to spherical particles, planar polymeric microstructures were prepared by emulsion polymerization using suitable UV curable comb-like branched surfactants. These planar microstructures were characterized by SEM. The EDX spectrometry showed that the planar particles were the latex particles with high C element content. It was different from the comparative KPS particle which had high K and S elements content. The UV curable comb-like emulsifiers synthesized in this study can be viewed as surfactant trimer with hydrophilic and hydrophobic blocks. The emulsifiers with bulky tail (suitable volume and functionality of the hydrophobic part) helped the formation of lamellar structure. The polymerizable emulsifiers copolymerized with the main monomer and become covalently bound to form an integral polymeric material. Hindered desorption of the emulsifier from the latex improved the latexes' stability and facilitate the formation of lamellar and oblate particles. This study provided a new approach to prepare lamellar particles and illustrated the correlation among the particle shape and the emulsifier structure. In order to control the shape of the latex particles, one has to be very careful about choosing the type of polymerizable emulsifiers and adjusting the reaction conditions.

Acknowledgements

The authors would like to thank the financial support from National Science Council under the contract of NSC-93-2218-E-035-011.

References

[1] Hansen FK. In: Daniels ES, Sudol EA, El-Aasser MS, editors. Polymer latexes. ACS symposium series, vol. 492. Washington, DC: American Chemical Society; 1992. p. 12.
[2] Holmberg K, Jonsson B, Kronberg B, Lindman B. Surfactants and polymers in aqueous solution. 2nd ed. England: Wiley; 2003 p. 74.
[3] Holmberg K, Jonsson B, Kronberg B, Lindman B. Surfactants and polymers in aqueous solution. 2nd ed. England: Wiley; 2003 p. 60–1.
[4] Tauer K, Goebel KH, Kosmella S, Stahler K, Neelsen J. Makromol Chem Macromol Symp 1990;31:107.
[5] Guyot A, Tauer K. Adv Polym Sci 1994;111:43.
[6] Green BW, Sheetz DP. J Colloid Interface Sci 1970;32:96.
[7] Green BW, Saunders FL. J Colloid Interface Sci 1970;33:393.
[8] Ottewill RH, Satgurunathan R. Colloid Polym Sci 1988;266:547.
[9] McGrath K, Drummond CJ. Colloid Polym Sci 1996;274:612.
[10] Biale J. US Patent 5,326,814; 1994.
[11] Onodera S, Yamamoto S, Tamai T, Takahashi H. Jpn Patent 06,239,908; 1994.
[12] Yokota K, Ichihara A, Shinike H. US Patent 5,324,862; 1994.
[13] Usai S. Jpn Patent 94/65,551; 1994.
[14] Kinoshita K. Jpn Patent 94/49,108; 1994.
[15] Cochin D, Laschewsky A, Nallet F. Macromolecules 1997;30:2278.
[16] Tsaur SL, Fitch RB. J Colloid Interface Sci 1987;115:450.
[17] Chen SA, Chang HS. J Polym Sci, Part A: Polym Chem 1985;23:2615.
[18] Bucsi A, Forcada J, Gibanel S, Heroguez V, Fontanille M, Gnanou Y. Macromolecules 1998;31:2087.
[19] Zana R. In: Holmberg K, editor. Novel surfactant. Surfactant science series, vol. 24. New York: Marcel Dekker; 1998. p. 241.
[20] Gibanel S, Forcada J, Heroguez V, Schappacher M, Gnanou Y. Macromolecules 2001;34:4451–8.
[21] Devinsky F, Lacko I, Iman T. J Colloid Interface Sci 1991;143:336.
[22] Laruelle G, Parvole J, Francois J, Billon L. Polymer 2004;45:5013.